Cellulose (2009) 16:587–597
DOI 10.1007/s10570-009-9306-0

Does the cellulose-binding module move on the cellulose surface?

Yu-San Liu · Yining Zeng · Yonghua Luo · Qi Xu · Michael E. Himmel · Steve J. Smith · Shi-You Ding

Received: 26 November 2008 / Accepted: 11 May 2009 / Published online: 19 June 2009

Abstract Exoglucanases are key enzymes required for the efficient hydrolysis of crystalline cellulose. It has been proposed that exoglucanases hydrolyze cellulose chains in a processive manner to produce primarily cellobiose. Usually, two functional modules are involved in the processive mechanism: a catalytic module and a carbohydrate-binding module (CBM). In this report, single molecule tracking techniques were used to analyze the molecular motion of CBMs labeled with quantum dots (QDs) and bound to cellulose crystals. By tracking the single QD, we observed that the family 2 CBM from *Acidothermus cellulolyticus* (*Ac*CBM2) exhibited linear motion along the long axis of the cellulose fiber. This apparent movement was observed consistently when different concentrations (25 μM to 25 nM) of *Ac*CBM2 were used. Although the mechanism of *Ac*CBM2 motion remains unknown, single-molecule spectroscopy has been demonstrated to be a promising tool for acquiring new fundamental understanding of cellulase action.

Y.-S. Liu · Y. Zeng · Y. Luo · Q. Xu · M. E. Himmel · S.-Y. Ding (✉)
Chemical and Biosciences Center, National Renewable Energy Laboratory, Golden, CO 80401, USA
e-mail: shi.you.ding@nrel.gov

S. J. Smith
Department of Electrical Engineering and Physics, South Dakota School of Mines, Rapid City, SD 57701, USA

Keywords Cellulose · Carbohydrate-binding module (CBM) · Single molecule spectroscopy

Introduction

Cellulose is a water insoluble polymer of β-1,4-linked cellobiose. In the cell walls of higher plants, it often forms a long bundle or fibrillar structure embedded into a matrix of other polysaccharides and lignin. Degradation of cellulose is a slow process that requires at least three types of enzymatic activities, the endoglucanase, which randomly breaks the internal β-1,4-glucosidic bonds and creates broken chain ends, and the exoglucanase, which cleaves the polymer from the ends to produce cellobiose. Finally, the beta-glucosidase hydrolyzes cellobiose to glucose, one of the most fermentable sugars obtainable from cell walls. It has been proposed that exoglucanases cleave the cellulose chain in a processive manner, which is believed to be critical for hydrolyzing crystalline cellulose efficiently. Biochemical studies have revealed that two functional modules are often required for an exoglucanse to function "processively." The catalytic modules (CM) of these enzymes always form an active tunnel in which the cellulose chain is precisely positioned, permitting hydrolysis of the glycosidic bond and release of cellobiose. The carbohydrate-binding module (CBM) functions as a binding unit to allow the enzyme to associate with the cellulose

surface. The CM and CBM are found to be linked directly with a linker polypeptide (e.g., the glycoside hydrolase family 7 cellobiohydrolase), or indirectly and associated with another proteins (e.g., scaffoldin of the cellulosome in some bacteria). Nevertheless, based on the hypothesis of the processive activity of exoglucanases, it appears that the CBM must be capable of translational movement along the cellulose surface to permit repeated hydrolysis cycles to occur. Preliminary results based on computer simulation have also suggested that the CBM is capable of movement along the cellulose surface (Bu et al. unpublished data). We report here an experimental study of the behavior of CBMs bound to crystalline cellulose surface using single molecule spectroscopy.

Ideal methodologies for analyzing biological systems dictate that the preparation and subsequent imaging change little or nothing about the molecular structure or chemistry of the specimen. Such methodologies exclude most high resolution microscopy techniques, yet are completely amenable to atomic force microscopy (AFM), nonlinear optics, and single molecule spectroscopy (SMS) (Ding et al. 2008, 2006). SMS refers to a set of spectroscopic approaches capable of investigating the dynamics and kinetics of each individual molecule. The common approach to SMS involves analyzing the electronic spectrum (fluorescence) or vibrational spectrum (infrared or Raman) under the manipulation of a specific key molecule that resides in the sample (Cornish and Ha 2007; Moerner 2007). Single-molecule fluorescence measurements have been used widely in the biological field to examine problems including: protein/RNA folding (Schuler et al. 2002; Zhuang and Rief 2003), diffusion analysis (Vrljic et al. 2005), DNA processing (Ha et al. 2002), DNA sequencing (Braslavsky et al. 2003), and cellular entry (Lakadamyali et al. 2003). Tracking the movement of a single molecule by fluorescence has also been used to investigate a variety of proteins or complexes, such as motor proteins (myosin V (Yildiz et al. 2003; Warshaw et al. 2005), myosin VI (Yildiz et al. 2004; Okten et al. 2004), kinesin (Yildiz et al. 2004; Nan et al. 2005), dynein (Nan et al. 2005)) and base-excision DNA-repair protein (human oxoguanine DNA glycosylase 1 (Blainey et al. 2006)). However, the use of SMS techniques to investigate cellulose degrading enzymes has not been reported.

CBMs are noncatalytic protein modules found in many carbohydrate-hydrolyzing enzymes, such as the cellulases and hemicellulases. They are thought to function as recognition modules that convey the catalytic modules of these enzymes to the target substrate, such as cellulose (Levy and Shoseyov 2002). Therefore, understanding the interaction between the CBM and the cellulose surface is critical for understanding overall cellulase action. Although the binding of the CBM with the cellulose surface has been shown by experiment to be essentially irreversible (the CBM is not lost to solution), logic dictates that one likely mode for catalysis requires that this domain translate on this surface. Jervis and coworkers demonstrated that Fluorescence Recovery after Photobleaching (FRAP) techniques could be used to suggest that cellulose binding domain of exoglycanase (CBD_{cex}) was capable of translation on the surface of crystalline cellulose 1β (Jervis et al. 1997). They further proposed that this movement was possible for CBD_{cex} both in an isolated form and as a module linked to a xylanase.

In order to evaluate SMS approaches for studying the binding and hydrolysis activities of cellulolytic enzymes, we have previously developed a system capable of self-assembly at the single molecule scale (Ding et al. 2006). In this system, CBMs were permitted to bind initially to *Valonia* cellulose crystals, followed by bio-conjugation with semiconductor QDs. These bio-assembles were then subjected to Total Internal Reflection Fluorescence (TIRF) microscopy and the concentrations of CBM and QD optimized to achieve single molecule resolution.

Materials and methods

Cloning and expression of CBMs

Two CBMs were used in this study, *Ac*CBM2 is a family 2 CBM from *Acidothermus cellulolyticus,* and *Ct*CBM3 is a family 3 CBM from *Clostridium thermocellum*. The detailed protocol for CBM cloning, expression, and purification was described in previous reports (Ding et al. 2006; Xu et al. 2009). Briefly, genomic DNAs of *A. cellulolyticus* and *C. thermocellum* were used as templates, and polymerase chain reaction (PCR) was used to amplify the

DNA fragments of CBMs. The primers used for PCR are 5′ GATATACATATGGGTGTGGCGTGCCGGG CGA 3′ and 5′ AGAGAGCTCGAGGCTGGCTGT GCAGCTGAGCGT 3′ for *Ac*CBM2; 5′ GATATAC ATATGGGCAATTTGAAGGTTGAAT 3′ and 5′ AGAGAGCTCGAGACCGGGTTCTTTACCCCA 3′ for *Ct*CBM3. All CBMs were cloned in pET28b(+) vector (Novagen, Madison, WI, USA) using restriction enzymes *Nde*I and *Xho*I to generate the expression plasmid pET-CBM that produces fusion protein with dual hexa-histidine-tag at its *N*- and *C*- termini. The CBMs were then over-expressed in *E. coli* strain of BL21 (DE3) (Stratagene, La Jolla, CA). Fusion proteins were purified using the QIAexpress Ni-NTA protein purification system (Qiagen, Valencia, CA). The CBM concentration was measured by NanoDrop 1000 (Thermo Scientific, Wilmington, DE, USA) and subsequently diluted with Tris buffer (50 mM Tris, pH 8.0) to optimize the resolution for single molecule detection.

Solubilization of QDs

The method used to solubilize QDs in water followed our previous report (Ai et al. 2007) using a mixture of *N*-acetyl-cysteine (NAC) and histidine (Sigma–Aldrich, St. Louis, MO). In brief, 100 μL of the TOP/TOPO (trioctylphosphine/trioctylphosphine oxide) capped (CdSe)ZnS core-shell QDs in toluene (Evident Technologies, Troy, NY) was added to 1.5 mL methanol and the mixture was centrifuged at 20,000×*g* for 15 min. The supernatant was discarded and the QD-containing pellet was washed with methanol three times and vacuum-dried. A 1.5 mL solution containing 62.5 mM each of histidine and NAC (Sigma–Aldrich, St. Louis, MO) (pH 8.1) was added to re-suspend the QD pellet with mild sonication. The NAC/histidine suspended QDs were centrifuged at 20,000×*g* for 15 min to remove un-reacted solid material. The approximate size of the TOP/TOPO QDs was 5.2 nm in diameter (Evident Technologies, Troy, NY) and the corresponding emission peak was 614 nm in toluene. The concentration of prepared NAC/histidine-capped QDs stock solution is estimated to be 200 nM according to the reported method (Yu et al. 2003), and it was subsequently diluted with the same NAC/histidine solution to optimize the resolution for single molecule detection.

Assembling CBMs, QDs, and cellulose crystals

The cellulose crystals used for this study were isolated from the green alga, *Valonia ventricosa* (Imai et al. 2003). Twenty micrograms of CBM (*Ac*CBM2 or *Ct*CBM3) protein in solution were incubated with 100 μg of *Valonia* cellulose crystals in 1 mL of Tris buffer (50 mM Tris, pH 8.0) by gentle mixing for 30 min; then followed by centrifugation (10,000×*g* for 3 min). These pellets were washed three times to remove unbound CBMs in the solution. The resulting CBM-bound-cellulose complexes were suspended in 500 μL Tris buffer. Ten microliters of the NAC/histidine-solubilized QDs solution were added to the cellulose/CBM suspensions. The QDs were then allowed to bind to the cellulose/CBM complexes by gently mixing. Unbound QDs were removed by repeated centrifugation and washing steps (using Tris pH 8.0). The final cellulose/CBM/QD conjugates were suspended in 50 μL Tris buffer. For single molecule detection, the concentrations of *Ac*CBM2 and QD were optimized to achieve single molecule resolution.

Förster resonance energy transfer (FRET)

FRET was used to further confirm the composition of the cellulose/*Ct*CBM3/QD constructs. QDs having an emission peak at 614 nm were used as the donor molecules and the Alexa 647 fluorescent dye (having an absorption peak at 647 nm and an emission peak at 668 nm) was used as the acceptor molecule. The anti-His tag antibody conjugate of the Alexa 647 fluorphore (Qiagen, Valencia, CA) was used to detect the histidine-tag of the *Ct*CBM3 protein. The antibody was then added to cellulose/*Ct*CBM3/QD suspensions (see above), and gently mixed for 1 hour in the dark and at room temperature. Unbound antibody was removed by repeated centrifugation and washing steps (using Tris pH 8.0). The final cellulose/*Ct*CBM3/QD/antibody conjugates were suspended in 50 μL Tris buffer for TIRF imaging. Spectra were recorded using a Fluorolog-3 spectrofluorometer (Horiba Jobin Yvon, Edison, NJ, USA) as previously reported (Ai et al. 2007).

Microscopic observation

TIRF microscopy (TIRF-M) was performed on an Olympus IX71 inverted microscope equipped with QuantEM: 512SC and CoolSNAP HQ^2 (Roper Scientific, Trenton, NJ, USA) cameras. Mercury lamp and a linearly polarized 488 nm argon laser (Melles Griot, Albuquerque, NM, USA) were used as the excitation sources. Several fluorescence filter sets were used for different purposes. For general fluorescence imaging, the Ex = 545–580 nm and Em = 610 LP nm filters were used for QDs. For single molecule detection, the Ex = 488/10X nm and Em = 650/50 M nm filters were used for QDs; in this case a band-pass filter (617/73) was placed before the camera to further suppress noise. For the FRET assay, the Ex = 488/10X nm and Em = 617/73 nm filters were used for QDs (donor); whereas the Ex = 488/10X nm and Em = 660 LP filters were used for the Alexa 647 dye (acceptor). Two objective lenses were used for these observations, the 150X lens (UApo, oil immersion and N.A. = 1.45) and the 100X lens (PlanApo, oil immersion and N.A. = 1.45). Freshly prepared samples (2-μL volume) were placed between two glass cover slips. After the sample spreads out by capillary effect, the cover slips were pressed together hard to minimize optical depth of the sample and to obtain a thin and even distribution of cellulose substrate fibers, maintained in an aqueous environment.

Single molecule tracking and data analysis

TIRF images were recorded as a sequence for later tracking analysis. Each sequence of images was analyzed by DIATRACK software (Semasopht, North Epping, Australia). All the spots on an image in the sequence were analyzed. Particular intensity thresholds were applied to exclude spots that were too bright (obvious aggregates containing multiple fluorphores). Each spot, which in most cases represents one single molecule, was fitted with a two-dimensional Gaussian function (Thompson et al. 2002). The centroid of a spot in one image was determined as the peak of the fitting Gaussian function. The centroid of the same spot throughout the sequence of images were determined from one frame to the next and finally reconstructed as a spatial trajectory recording the movement of the spot. The accuracy of determining a centroid was primarily limited by the number of photons collected from the particular spot. The extracted data was processed with custom MATLAB (MathWorks, Natick, MA, USA) script.

Results and discussions

Cellulose/CBM/QD constructs

In our previous work (Ding et al. 2006; Xu et al. 2009), we developed a method to use QDs to label the CBM that specifically binds to the planar face of crystalline cellulose. The Type-A surface-binding CBMs (*Ct*CBM3 and *Ac*CBM2) that have high affinity for crystalline cellulose (Tormo et al. 1996; Morag et al. 1995) were used in this study. QDs were conjugated to CBMs using dual histidine-tags introduced genetically to the *N*- and *C*-termini of the CBM molecule (Fig. 1). Although the QDs and CBMs are of about the same size (5 nm in diameter), simply labeling one CBM with one QD initially and then applying this assembly to cellulose would generate large QD-CBM aggregates. This approach would also make it more difficult to arrange the QD-CBM aggregates on the cellulose (data not shown). In practice then, the CBMs were deposited onto cellulose first and then subsequently labeled with the QDs in a two-step procedure (Ding et al. 2005). Typical fluorescence images of the cellulose/*Ct*CBM3/QD conjugates are shown in Fig. 2a. All QDs were found to be specifically aligned on the cellulose crystals. After labeling the cellulose/*Ct*CBM3 with QDs, we

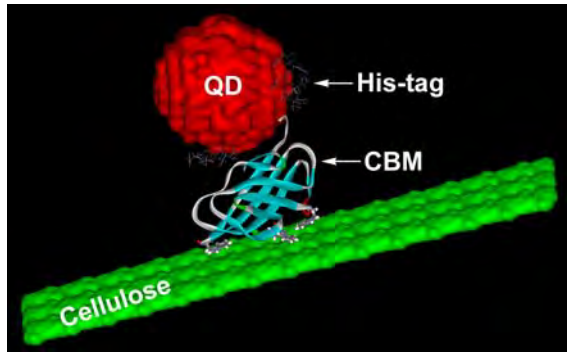

Fig. 1 Cartoon showing the cellulose/*Ac*CBM2/QD system. The *Ac*CBM2 facilitates binding to the cellulose substrate. QDs are anchored to the *Ac*CBM2 protein by the dual histidine-tags (*His-tag*) and fused at *N*- and *C*-termini

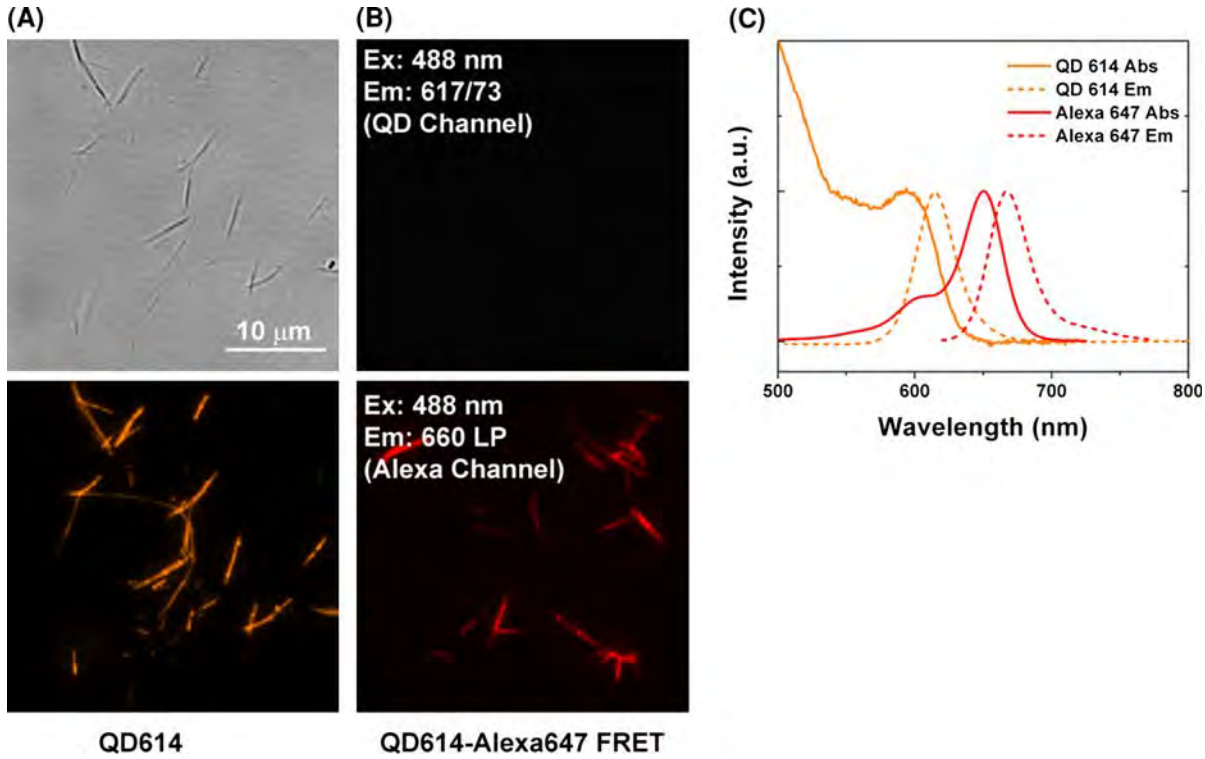

Fig. 2 Photomicrographic images of fluorescently tagged *Ct*CBM3 on *Valonia* cellulose. **a** QDs are anchored on *Ct*CBM3 proteins by the histidine-tags fused at both *N*- and *C*-termini. Bright field image on the *top* showing cellulose, and fluorescence image in the *bottom panel*; **b** images obtained from the microscope channels transmitting only QD (*top*) and Alexa (*bottom*) fluorescence, respectively. The excitation laser wavelength 488 nm can only excite QD but not Alexa. The absence of QD fluorescence in the *top* image and the presence of Alexa fluorescence in the *bottom* show that QD (donor, emission peak at 614 nm) energy has transferred to Alexa dye (acceptor, absorption peak at 647 nm). Anti-His tag antibody conjugate Alexa fluorphore detects histidine-tagged *Ct*CBM3 protein indicating QD bind to cellulose directed by CBM; **c** absorption and emission spectra of QD614 (*orange line*) and Alexa fluorphore (*red line*)

further used monoclonal antibody (anti-His tag antibody) conjugated with Alexa 647 fluorphore to detect histidine-tagged *Ct*CBM3 protein. FRET imaging was then used to confirm the assembly of the cellulose/*Ct*CBM3/QD constructs. In this system, the QD 614 (donor) has broad excitation spectra and a narrow emission peak at 614 nm. The Alexa 647 (acceptor) has an absorption peak at 647 nm and emission peak at 668 nm. A 488 nm laser was used to excite the QDs and two band-pass filter sets (660 LP and 617/73) were used to detect the emissions of Alexa 647 and QD 614, respectively. Figure 2b shows the FRET images of these two channels. Indeed, only emission from Alexa 647 could be detected when the 488 nm laser was used to excite the QD, which indicated high FRET efficiency from the QD to the Alexa fluorphore. FRET imaging provided direct evidence that QD-CBM conjugation was facilitated by the interaction between the dual histidine tags of the engineering CBM and the zinc (II) atoms on the QD surface (Goldman et al. 2005; Slocik et al. 2002). In our previous work (Xu et al. 2009), we observed that the arrangement of *Ac*CBM2/QD binding to cellulose appeared more regularly than that of *Ct*CBM3/QD. Preliminary microscopic tracking also exhibited more complicated modes of motion of *Ct*CBM3/QD bound to cellulose (data not shown). Therefore, in this report, we focused on *Ac*CBM2/QD for all 2-D tracking experiments.

Optimization of QD concentration

In order to track the molecule behavior of the CBMs on cellulose surfaces, the first challenge was to ensure

that sample preparation achieved single molecule dispersion. Here, the concentration of target molecules plays a vital role (Gopich 2008; Steinmeyer et al. 2005). We found that the target molecules must be diluted sufficiently to achieve single molecule dispersion. However, it is likely that using very low concentrations could increase signals generated by impurities (background signals), thus reducing the accuracy of the centroidal determination.

In this study, concentrated *Ac*CBM2 (25 μM) was used initially to ensure saturated binding of the protein to cellulose. This minimizes potential non-specific binding between QD and cellulose. Solutions of QDs in concentrations ranging from 200 nM to 1 pM were then added to the *Ac*CBM2-bound cellulose to obtain the appropriate QD concentration range (determined earlier to be ideal for observing single QD particles). As shown in Fig. 3, the intensity of overall QD fluorescence decreases with decreasing QD concentration. In Fig. 3a, QDs were excited using the 488 laser that illuminated the entire cellulose crystal. The single molecule level of detection was achieved by diluting QDs to 100 pM (Fig. 3b) and even to 50 pM (Fig. 3c); however, further dilution of the QDs to 1 pM (Fig. 3d) did not yield detectable fluorescence signal even with strong excitation. Thus, QD concentrations in the picomole range appeared to be suitable for single molecule imaging of the cellulose/*Ac*CBM2/QD614 system.

The accuracy in the centroid determination is calculated by the following formula (Thompson et al. 2002):

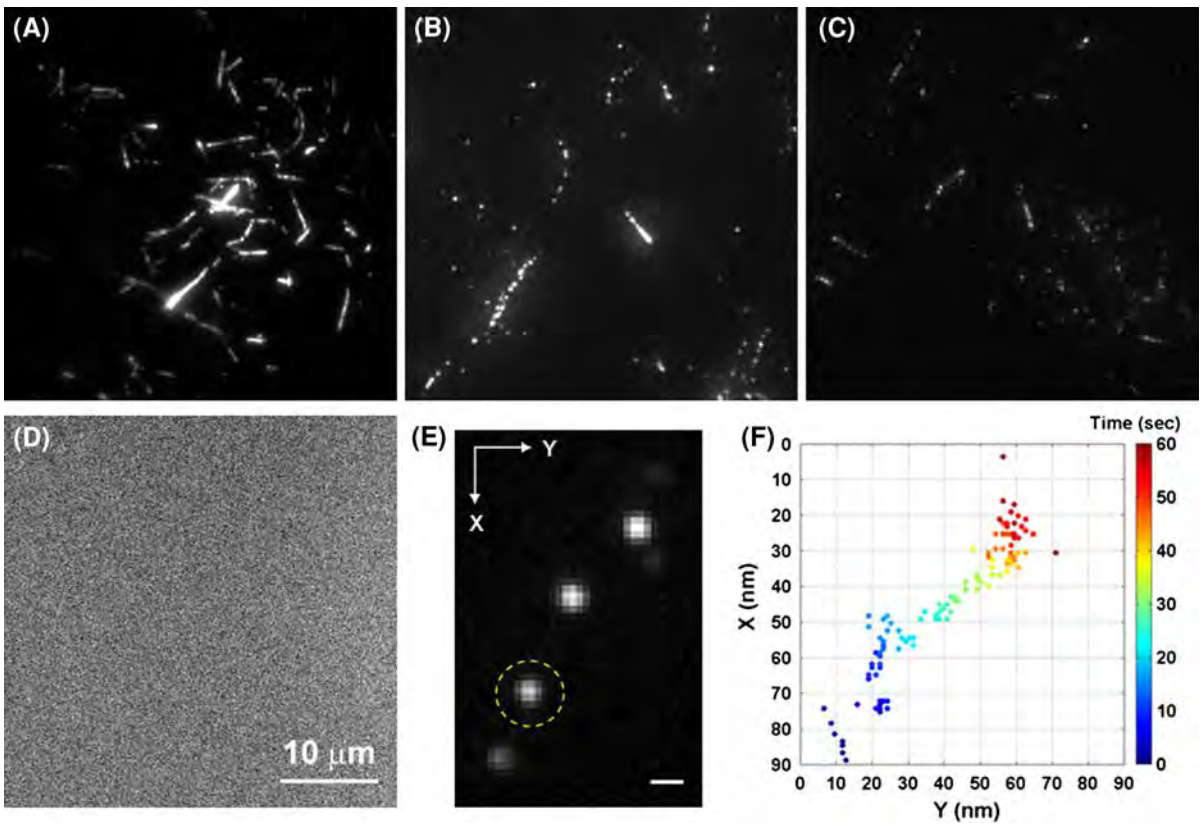

Fig. 3 Total internal reflection fluorescence micrographs of cellulose crystals labeled by *Ac*CBM2 and QD614 with various QD concentrations. QDs appear as *white spots*. *Ac*CBM2 concentration was fixed at 25 μM with QD concentration at (**a**) 200 nM (**b**)100 pM (**c**)50 pM (**d**)1 pM. Individual *dots* can be resolved in the images with 100 pM and 50 pM QD concentration. (**e**) A single image of QD (100 pM) tagged *Ac*CBM2 (25 μM) on cellulose from a 120-frame sequence acquired at 2 Hz frame rate. Four QDs lined up on the cellulose. The *circled* molecule was selected for tracking study. Scale *bar* 500 nm. (**f**) A typical trajectory demonstrated *Ac*CBM2 moving along the direction of the cellulose crystal. The color coded *bar* represents time scale of 60 s

$$\sigma \approx \sqrt{\frac{1}{N}\left(s^2 + \frac{a^2}{12}\right)}$$

where s is the width of diffraction limited spot (212 nm), a is the pixel size (104 nm without binning), and N is the number of photons detected. In this study, two concentrations of QDs (100 pM and 50 pM) were used to test the accuracy of above calculation. We noted that QD concentrations of 50 pM required more photoactivation (e.g., $\sim$1 min) before being observable as reported previously (Sun et al. 2006; Silver and Ou 2005). We therefore defined 100 pM as our optimal QD condition for tracking potential movement. Because, we used a back-illumination CCD camera with on-chip gain capability, N is determined from the image as:

$$\mathrm{N} = \frac{I \times g}{G}$$

where I is the spot intensity measured by defining a spot with an 11 × 11 pixel region after subtracting background, g is the conversion gain that indicates the number of photoelectrons per analogue-digital converter unit (ADU) and G is the on-chip gain factor. We used values of $g = 6\ \mathrm{e}^-/\mathrm{ADU}$ and $G = 200$. Using a typical excitation power of 3 mW (after objective) and 500–2,000 ms of exposure time, we usually obtained about 1,500–3,000 photons from each spot. The error in the centroid determination was then calculated as about 4–5.5 nm.

Observation of single *Ac*CBM2 molecules on cellulose

A QD concentration of 100 pM was used to analyze the trajectory of QDs in the cellulose/*Ac*CBM2/QD system. Based on our FRET imaging, it appeared that all QDs were bound tightly to the CBM. By visualizing the movement of the QDs, we could observe indirectly *Ac*CBM2 behavior on cellulose. Figure 3e shows a representative image from a sequence movie (corresponding to 120 frames with 2 Hz frame rate) of a cellulose crystal on which four single QDs/*Ac*CBM2 were observed. The circled QD in Fig. 3e was used for tracking molecular movement, and its tracking result was shown as Fig. 3f. The trajectory indicated that these QDs appeared to be moving directionally along the cellulose long axis. In this case, the motion was almost linear and was confined in 1-dimension during the 60 s observation. The observed movement of the CBM may be the combination of Brownian motion and translational motion along the cellulose surface. We speculate that in short time scale, i.e., few seconds, CBM molecules move randomly primarily due to Brownian motion, the translational motion may or may not be captured, or may be difficult to differentiate from Brownian motion. However, in tens of seconds or longer time scale, the observed movement of CBM molecules should be predominated by translational motion, which showed in Fig. 3f.

Control experiments were conducted to further confirm that these apparent motions indeed resulted from the movement of *Ac*CBM2. An important question was whether or not the apparent motion observed was affected by the concentration of the *Ac*CBM2. The number of the CBM molecules bound on the cellulose surface could affect the intervals between CBMs and hence affect the apparent distance traveled by the CBMs. A dense arrangement of CBMs (i.e., concentrated CBMs) along the cellulose crystal might limit the available space and constrain CBM movement. Using the optimal QD concentration determined earlier, 100 pM, the *Ac*CBM2 solution was diluted from 25 μM (Fig. 3b) to 25 nM (Fig. 4a) and 250 pM (Fig. 4b) to generate the cellulose/*Ac*CBM2/QDs system. In Fig. 4a, QDs in this system can be observed on individual cellulose crystals where they "line up" in the long axis dimension of the crystal. In Fig. 4b, few QDs can be seen on single cellulose crystals; most of them show up on cellulose bundles. The tracking of diluted *Ac*CBM2 movement was conducted using solutions of 25 nM *Ac*CBM2 and 100 pM QDs (same as the condition in Fig. 4a). The trajectory determined (see Fig. 4c) demonstrated the QDs displayed very similar patterns of motion, which was linear and directional along the long axis of the cellulose crystal during the 60 sec observation.

Another important question was whether or not the nonspecific binding of QDs on cellulose could result in directional movement. In order to answer this question, we further performed a control experiment in which the QDs were mixed with the cellulose crystals directly without adding *Ac*CBM2, all other conditions were the same as above. In this case, very few QDs could be found on the single cellulose crystals, although there

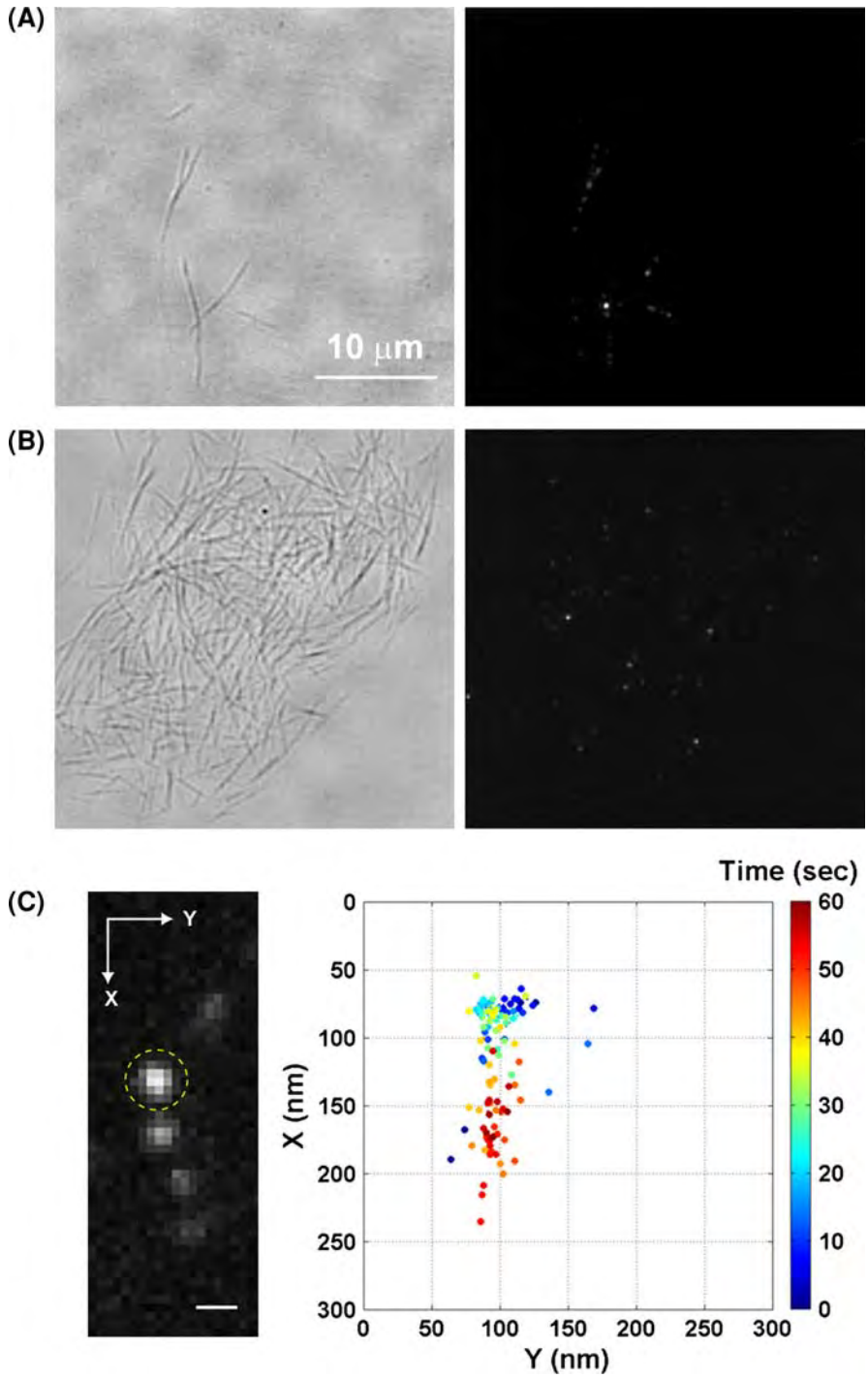

Fig. 4 Total internal reflection fluorescence micrographs of cellulose crystals labeled by *Ac*CBM2 and QD614 with various *Ac*CBM2 concentrations. QD concentration was fixed at 100 pM with *Ac*CBM2 concentration at (**a**) 25 nM (B) 250 pM. QDs appear as *white spots* in the *bottom row* whereas bright field images showing the cellulose crystals are in the *top row*. QDs can be seen on single cellulose crystals in (**a**) and in cellulose bundles in (**b**). (**c**) (*Left*) A single image of QD (100 pM) tagged *Ac*CBM2 (25 nM) on cellulose from a 150-frame sequence acquired at 2.5 Hz frame rate (same condition as Fig. 4a). The *circled* molecule was selected for tracking. Scale *bar* 500 nm. (*Right*) The trajectory demonstrated CBM moving in 1-D along the cellulose direction. The color coded *bar* represents time scale of 60 s

were still some QDs nonspecifically bound to cellulose bundles, as shown in Fig. 5a. The trajectory of a single, isolated QD is shown in Fig. 5b. Here, the nonspecifically-bound QDs moved randomly. Note that this motion did not at all compare to the highly vectored, and progressive *Ac*CBM2-driven QDs shown in Figs 3e and 4c. This experiment thus confirmed that the directional motion of QDs was indeed driven by CBM. However, the apparent distances moved for the cellulose/*Ac*CBM2/QD and cellulose/QD systems

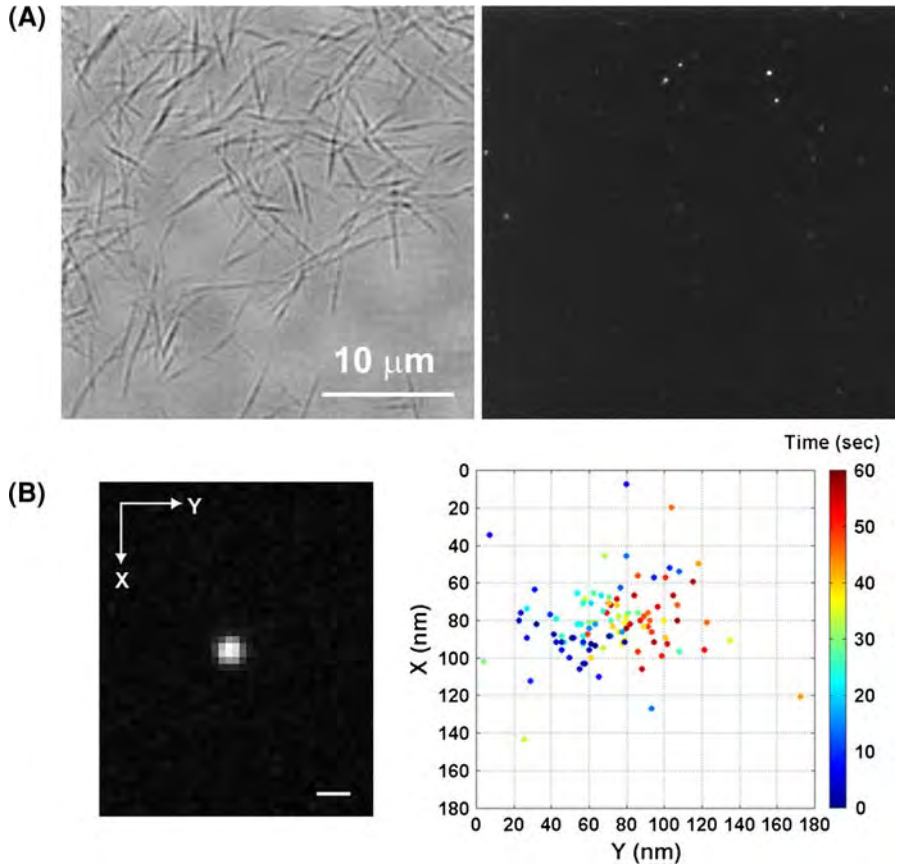

Fig. 5 **a** Total internal reflection fluorescence micrograph of cellulose crystals non-specifically labeled with QD (100 pM). Bright field image showed cellulose crystal bundles (*left*). QDs appear as *white spots* (*right*); **b** (*left*) a single image of QD (100 pM) non-specifically bound to cellulose from a 150-frame sequence acquired at 2.5 Hz frame rate. Scale *bar* 500 nm. (*Right*) The trajectory demonstrated QD movement is not as narrowly confined on the cellulose crystal. The color coded *bar* represents time scale of 60 s

were not significantly different, which may imply that the overall resolution obtained from the current instrumental setup (e.g., laser, N.A. of objective lenses, microscope layout, etc.) was not optimized to quantitatively analyze the actual motion of CBM. Nevertheless, the results presented here clearly show that single QD movement driven by CBM conjugation display different characteristics than do free QDs (non-specifically bound to cellulose). We also noted that the observed *Ac*CBM2 movement was consistent with a previous report regarding CBD_{cex} bound on crystal cellulose (Jervis et al. 1997). Preliminary results of computer simulation also suggest CBM may move in a repetition of small steps corresponding to cellobiose units (Bu et al. unpublished data). The driving force for CBM motion is still unknown and its underlying mechanism needs more experimental clarification.

Another possible artifact which may explain this apparent movement is the intermittency of energy emission (blinking) from two (or more) QDs lying in one diffraction-limited spot. Unlike conventional dye molecules, which have simple on-off emission patterns, single QDs can exhibit multiple levels of emission. In other words, the apparent intensity of QDs luminescence may vary continuously; the blinking phenomenon is thus not a good indicator for identifying single dots (Kai et al. 2006). We noted that the one-dimensional trajectory provided an accurate position of the QD as a function of time, based on the observations for the case of the QD/*Ac*CBM2/cellulose system (Figs 3, 4). The QD trajectory data shown here have clearly demonstrated that the motion of *Ac*CBM2/QD is linear and directional along the long axis of the cellulose crystal. With the current microscopic setup, it does not allow us to quantitatively subtract the instrument shift from the tracking of CBM movement. Compared to the control experiment that has QD non-specific bound to celluloses showed random, non-directional movement, we therefore believe the observed motion is driven by CBM motion.

Conclusion

The single molecule spectroscopy approach was used to analyze the bacterial family 2 CBM (*Ac*CBM2) labeled by QDs and bound to cellulose. By tracking the QDs single molecules; we have demonstrated that the *Ac*CBM2 exhibits a linear and directional motion along the cellulose crystal, which was not observed in the case of QDs nonspecifically bound to cellulose. Due to the limited resolution of the current optical microscope setup used, we were not able to analyze the velocity of the CBM motion, nor the distance that the CBM is able to move. Future improvements in instrumental resolution are required to further describe the mechanism of *Ac*CBM2 binding to cellulose. We believe that the single molecule approach used here offers new opportunities to guide us toward the fundamental understanding of cellulase function, specifically the mechanism of the exoglucanase "processivity."

Acknowledgments The authors thank Dr. Haw Yang and his group at University of California at Berkeley for valuable discussions. The authors gratefully acknowledge the US Department of Energy, Office of Energy Efficiency and Renewable Energy Biomass Program for support of the work to develop quantum dot conjugates and support from the DOE Office of Science, Office of Biological and Environmental Research through the BioEnergy Science Center (BESC), a DOE Bioenergy Research Center, for the work on single molecule visualization and analysis.

References

Ai X, Xu Q, Jones M, Song Q, Ding SY, Ellingson RJ, Himmel M, Rumbles G (2007) Photophysics of (CdSe) ZnS colloidal quantum dots in an aqueous environment stabilized with amino acids and genetically-modified proteins. Photochem Photobiol Sci 6(9):1027–1033. doi:10.1039/b706471c

Blainey PC, van Oijent AM, Banerjee A, Verdine GL, Xie XS (2006) A base-excision DNA-repair protein finds intrahelical lesion bases by fast sliding in contact with DNA. Proc Natl Acad Sci USA 103(15):5752–5757. doi:10.1073/pnas.0509723103

Braslavsky I, Hebert B, Kartalov E, Quake SR (2003) Sequence information can be obtained from single DNA molecules. Proc Natl Acad Sci USA 100(7):3960–3964. doi:10.1073/pnas.0230489100

Cornish PV, Ha T (2007) A survey of single-molecule techniques in chemical biology. ACS Chem Biol 2(1):53–61. doi:10.1021/cb600342a

Ding SY, Smith S, Xu Q, Sugiyama J, Jones M, Rumbles G, Bayer EA, Himmel ME (2005) Ordered arrays of quantum dots using cellulosomal proteins. Ind Biotechnol 1:198–206. doi:10.1089/ind.2005.1.198

Ding SY, Xu Q, Ali MK, Baker JO, Bayer EA, Barak Y, Lamed R, Sugiyama J, Rumbles G, Himmel ME (2006) Versatile derivatives of carbohydrate binding modules for imaging of complex carbohydrates approaching the molecular level of resolution. Biotechniques 41:435–443. doi:10.2144/000112244

Ding SY, Xu Q, Crowley M, Zeng Y, Nimlos M, Lamed R, Bayer EA, Himmel ME (2008) A biophysical perspective on the cellulosome: new opportunities for biomass conversion. Curr Opin Biotechnol 19(3):218–227. doi:10.1016/j.copbio.2008.04.008

Goldman ER, Medintz IL, Hayhurst A, Anderson GP, Mauro JM, Iverson BL, Georgiou G, Mattoussi H (2005) Self-assembled luminescent CdSe-ZnS quantum dot bioconjugates prepared using engineered poly-histidine terminated proteins. Anal Chim Acta 534(1):63–67. doi:10.1016/j.aca.2004.03.079

Gopich IV (2008) Concentration effects in "Single-Molecule" spectroscopy. J Phys Chem B 112(19):6214–6220. doi:10.1021/jp0764182

Ha T, Rasnik I, Cheng W, Babcock HP, Gauss GH, Lohman TM, Chu S (2002) Initiation and re-initiation of DNA unwinding by the *Escherichia coli* Rep helicase. Nature 419(6907):638–641. doi:10.1038/nature01083

Imai T, Putaux JL, Sugiyama J (2003) Geometric phase analysis of lattice images from algal cellulose microfibrils. Polymer 44(6):1871–1879. doi:10.1016/S0032-3861(02)00861-3

Jervis EJ, Haynes CA, Kilburn DG (1997) Surface diffusion of cellulases and their isolated binding domains on cellulose. J Biol Chem 272(38):24016–24023. doi:10.1074/jbc.272.38.24016

Kai Z, Hauyee C, Aihua F, Alivisatos AP, Haw Y (2006) Continuous distribution of emission states from single CdSe/ZnS quantum dots. Nano Lett 6(4):843–847. doi:10.1021/nl060483q

Lakadamyali M, Rust MJ, Babcock HP, Zhuang XW (2003) Visualizing infection of individual influenza viruses. Proc Natl Acad Sci USA 100(16):9280–9285. doi:10.1073/pnas.0832269100

Levy I, Shoseyov O (2002) Cellulose-binding domains biotechnological applications. Biotechnol Adv 20(3–4):191–213. doi:10.1016/S0734-9750(02)00006-X

Moerner WE (2007) Single-molecule chemistry and biology special feature: new directions in single-molecule imaging and analysis. Proc Natl Acad Sci USA 104(31):12596–12602. doi:10.1073/pnas.0610081104

Morag E, Lapidot A, Govorko D, Lamed R, Wilchek M, Bayer EA, Shoham Y (1995) Expression, purification, and characterization of the cellulose-binding domain of the scaffoldin subunit from the cellulosome of *Clostridium thermocellum*. Appl Environ Microbiol 61(5):1980–1986

Nan XL, Sims PA, Chen P, Xie XS (2005) Observation of individual microtubule motor steps in living cells with endocytosed quantum dots. J Phys Chem B 109(51):24220–24224. doi:10.1021/jp056360w

Okten Z, Churchman LS, Rock RS, Spudich JA (2004) Myosin VI walks hand-over-hand along actin. Nat Struct Mol Biol 11(9):884–887. doi:10.1038/nsmb815

Schuler B, Lipman EA, Eaton WA (2002) Probing the free-energy surface for protein folding with single-molecule

fluorescence spectroscopy. Nature 419(6908):743–747. doi:10.1038/nature01060

Silver J, Ou W (2005) Photoactivation of quantum dot fluorescence following endocytosis. Nano Lett 5(7):1445–1449. doi:10.1021/nl050808n

Slocik JM, Moore JT, Wright DW (2002) Monoclonal antibody recognition of histidine-rich peptide encapsulated nanoclusters. Nano Lett 2(3):169–173. doi:10.1021/nl015706l

Steinmeyer R, Noskov A, Krasel C, Weber I, Dees C, Harms GS (2005) Improved fluorescent proteins for single-molecule research in molecular tracking and co-localization. J Fluoresc 15(5):707–721. doi:10.1007/s10895-005-2978-4

Sun YH, Liu YS, Vernier PT, Liang CH, Chong SY, Marcu L, Gundersen MA (2006) Photostability and pH sensitivity of CdSe/ZnSe/ZnS quantum dots in living cells. Nanotechnology 17(17):4469–4476. doi:10.1088/0957-4484/17/17/031

Thompson RE, Larson DR, Webb WW (2002) Precise nanometer localization analysis for individual fluorescent probes. Biophys J 82(5):2775–2783. doi:10.1016/S0006-3495(02)75618-X

Tormo J, Lamed R, Chirino AJ, Morag E, Bayer EA, Shoham Y, Steitz TA (1996) Crystal structure of a bacterial family-III cellulose-binding domain: a general mechanism for attachment to cellulose. EMBO J 15(21):5739–5751

Vrljic M, Nishimura SY, Moerner WE, McConnell HM (2005) Cholesterol depletion suppresses the translational diffusion of class II major histocompatibility complex proteins in the plasma membrane. Biophys J 88(1):334–347. doi:10.1529/biophysj.104.045989

Warshaw DM, Kennedy GG, Work SS, Krementsova EB, Beck S, Trybus KM (2005) Differential Labeling of myosin V heads with quantum dots allows direct visualization of hand-over-hand processivity. Biophys J 88(5):L30–L32. doi:10.1529/biophysj.105.061903

Xu Q, Tucker MP, Arenkiel P, Ai X, Rumbles G, Sugiyama J, Himmel ME, Ding SY (2009) Labeling the planar face of crystalline cellulose using quantum dots directed by type-I carbohydrate-binding modules. Cellulose 16(1):19–26

Yildiz A, Forkey JN, McKinney SA, Ha T, Goldman YE, Selvin PR (2003) Myosin V walks hand-over-hand: single fluorophore imaging with 1.5-nm localization. Science 300(5628):2061–2065. doi:10.1126/science.1084398

Yildiz A, Park H, Safer D, Yang ZH, Chen LQ, Selvin PR, Sweeney HL (2004a) Myosin VI steps via a hand-over-hand mechanism with its lever arm undergoing fluctuations when attached to actin. J Biol Chem 279(36):37223–37226. doi:10.1074/jbc.C400252200

Yildiz A, Tomishige M, Vale RD, Selvin PR (2004b) Kinesin walks hand-over-hand. Science 303(5658):676–678. doi:10.1126/science.1093753

Yu WW, Qu LH, Guo WZ, Peng XG (2003) Experimental determination of the extinction coefficient of CdTe, CdSe, and CdS nanocrystals. Chem Mater 15(14):2854–2860. doi:10.1021/cm034081k

Zhuang XW, Rief M (2003) Single-molecule folding. Curr Opin Struct Biol 13(1):88–97. doi:10.1016/S0959-440X(03)00011-3